NASA Technical Memorandum 103258
AIAA 90-2268

Hot Gas Ingestion Test Results of a Two-Poster Vectored Thrust Concept With Flow Visualization in the NASA Lewis 9- by 15-Foot Low Speed Wind Tunnel

Albert L. Johns, George Neiner, and Timothy J. Bencic
Lewis Research Center
Cleveland, Ohio

and

Joseph D. Flood, Kurt C. Amuedo, and Thomas W. Strock
McDonnell Douglas Corporation
St. Louis, Missouri

Prepared for the
26th Joint Propulsion Conference
cosponsored by the AIAA, SAE, ASME, and ASEE
Orlando, Florida, July 16-18, 1990

NASA

HOT GAS INGESTION TEST RESULTS OF A TWO-POSTER VECTORED THRUST CONCEPT WITH FLOW VISUALIZATION IN THE NASA LEWIS 9- BY 15-FOOT LOW SPEED WIND TUNNEL

Albert L. Johns, George Neiner, and Timothy J. Bencic
National Aeronautics and Space Administration
Lewis Research Center
Cleveland, Ohio 44135

and

Joseph D. Flood, Kurt C. Amuedo, and Thomas W. Strock
McDonnell Aircraft Company
McDonnell Douglas Corporation
St. Louis, Missouri 63166

SUMMARY

A 9.2 percent scale Short Takeoff and Vertical Landing (STOVL) hot gas ingestion model was designed and built by McDonnell Douglas Corporation (MCAIR) and tested in the NASA Lewis Research Center 9- by 15-Foot Low Speed Wind Tunnel (LSWT). Hot gas ingestion, the entrainment of heated engine exhaust into the inlet flow field, is a key development issue for advanced short takeoff and vertical landing aircraft. This paper covers flow visualization from the phase I test program, conducted by NASA Lewis Research Center and McDonnell Douglas Corporation, which evaluated the hot ingestion phenomena and control techniques. The phase II test program, which was conducted by Lewis Research Center, evaluated the hot gas ingestion phenomena at higher temperatures and used a laser sheet to investigate the flow field.

Hot gas ingestion levels were measured for the several forward nozzle splay configurations and with flow control/lift improvement devices (LIDs) which reduced the hot gas ingestion. The model support system had four degrees of freedom - pitch, roll, yaw, and vertical height variation. The model support system also provided heated high-pressure air for nozzle flow and a suction system exhaust for inlet flow. The test was conducted at full scale nozzle pressure ratios and inlet Mach numbers.

This paper documents test and data analysis results from phase II and flow visualization from both phase I and II. A description of the model and facility modifications is also provided. Headwind velocity was varied from 10 to 23 kn. Results are presented over a range of nozzle pressure ratios at a 10-kn headwind velocity. The phase II program was conducted at exhaust nozzle temperatures up to 1460 °R and utilized a sheet laser system for flow visualization of the model flow field in and out of ground effects. The results reported herein are for nozzle exhaust temperatures up to 1160 °R. These results contain the compressor face pressure and temperature distortions, the total pressure recovery, the inlet temperature rise, and the environmental effects of the hot gas. The environmental effects include the ground plane contours, the model airframe heating, and the location of the ground flow separation.

INTRODUCTION

Advanced Short Takeoff and Vertical Landing (STOVL) aircraft are being considered for operation around the turn of the century. In order to meet this target, the technologies critical to the successful operation of the STOVL concepts must be resolved. One of the critical technologies associated with the vectored lift concept is that of hot gas ingestion (HGI) while an aircraft is in ground effects (refs. 1 and 2).

Hot gas ingestion can be categorized as near field and far field phenomena (fig. 1). The near field hot gas problem occurs when two or more hot exhaust jets impinge on the ground and radiate in all directions until one jet encounters another jet. When these jets meet, a fountain is formed. This fountain can hit the undersurface of the fuselage and run forward into the inlet flow field. The hot air, once ingested, can result in both compressor temperature and pressure distortions and loss in engine thrust and/or stall. The near field hot gas ingestion is generally the primary source of the hot gas ingestion. The near field hot gas ingestion is a function of the model height (main landing gear wheel height) above the ground plane (ref. 3). The far field hot gas ingestion occurs when the ground jet from the nozzle(s) flow separates from the ground ahead of the model and gets blown back into the inlet flow field. The far field hot gas ingestion is a function of the headwind velocity. The magnitude of the far field hot gas ingestion is greatly reduced in comparison to the near field ingestion because the exhaust jet flow mixes with the ambient air flow.

This paper presents results from phase I and phase II obtained at the compressor face of a 9.2 percent scale vectored thrust STOVL model in ground effects. The STOVL model had a unique model support system with four degrees of freedom (pitch, roll, yaw, and vertical height variation), heated high-pressure air for nozzle flow, and a suction system exhaust for inlet flow. During phase I testing the model support system was operated manually. However, phase II testing had the model integrated support system (MISS), which was operated remotely from the control room. For the purpose of this report, only the height variation was used on the MISS. The pitch, roll, and yaw were set initially and kept constant thereafter. The hot gas ingestion results are shown for a headwind (free-stream) velocity of 10 kn. The near and far field sheet laser flow visualization are presented for the span and streamwise laser positions.

FACILITY, MODEL CONFIGURATIONS, AND SUPPORT SYSTEM

The NASA Lewis 9- by 15-Foot Low Speed Wind Tunnel (LSWT) was used to develop the hot gas ingestion database. The 9- by 15-ft LSWT, constructed within the return leg of the 8- by 6-Foot Supersonic Wind Tunnel (SWT), is shown schematically in figure 2. Tunnel velocities from 8 to 23 kn were set by using the air dryer blowers and doors 4 and 5.

A schematic for the HGI model, MCAIR model 279-3C, is shown in figure 3. The model consisted of five major subassemblies: the forward fuselage, the center fuselage, the aft fuselage, the wings, and the canards. The forward fuselage contained the main inlet and a translating cowl auxiliary inlet which made up the bifurcated inlet system. The inlet suction duct was part of the suction system and was used to create inlet (compressor face) flow. The

center fuselage contained the nozzle system, and high-pressure hot-air lines supplied hot air (up to 1460 °R) to the model's four nozzles. Lift improvement devices (LID's) could also be attached to the center fuselage.

The LID's consisted of longitudinal strakes, sidewalls, a forward fence, and an aft fence (optional). They generally enclosed the forward and aft pairs of nozzles. The undersurface of the HGI model with the 0° forward nozzle splay configuration is shown in figure 3.

The forward nozzle splay angle is defined in figure 4(a). The splay angle was measured with reference to a vertical line through the nozzle centerline. A negative splay means the nozzles are in-board of the vertical line.

The nozzle vector thrust angle is shown in figure 4(b). The nozzle vector angle for the data presented in this paper is 82° on the forward nozzles and 83.5° on the aft nozzles. The model was capable of vectoring thrust from 0° (full aft) to 110° (slightly forward).

MODEL INSTALLED IN THE 9- BY 15-FOOT LOW SPEED WIND TUNNEL

A schematic of the installation of the 9.2 percent scale model and the supporting system in the 9- by 15-Foot Low Speed Wind Tunnel (LSWT) are shown in figure 5. The supporting system includes a remotely controlled model integrated support system (MISS) that had four degrees of freedom (model height, yaw, pitch, and roll). Figure 6(a) shows the model and MISS installed in the 9- by 15-ft LSWT. A ground plane was installed with static pressures, air temperature instrumentation, and boundary-layer rakes. The ground plane had a sliding trap door that was open when the nozzle conditions were being set and closed to set up the steady state conditions during data recording. For hot gas ingestion testing, the section of the trap door under the model was covered with flat pieces of shuttle tiles. The tiles were used so the structure of the trap door would not see the 1460 °R nozzle airflow temperature. When laser sheet testing was conducted, the tiles were covered with a thin stainless steel sheet to prevent water, used for flow visualization, from damaging the tiles and trap door instrumentations. Figure 6(b), an aft view of the installation in the 9- by 15-ft LSWT, shows the ground plane ejector system which evacuated the hot exhaust gases from the vicinity of the model when the nozzle flow conditions were being set. The ejectors were automatically shut off when the trap door closed.

Two heaters were used for the 1460 °R nozzle airflow temperature. One heater supplied airflow for the front nozzles, and the other heater supplied airflow for the aft nozzles. Each heater is capable of delivering 1560 °R process air at 5 lb/sec and 450 psig.

A copper metal vapor laser described in the LASER SHEET FLOW VISUALIZATION Section) was used to generate the illumination system for the flow field. The laser and turn key control system are shown in figure 7.

A schematic of the ground plane is shown in figure 8. The ground plane was 336 in. long, 176 in. wide, and 18 in. off the wind tunnel floor. The

trap door opening was 42 in. in the axial direction and 40.75 in. in the span direction. The trap door closed from a full open position in 0.5 sec.

A cross section view of the test section is shown in figure 9. The test section was normally lined with an acoustic treatment. For the hot gas ingestion tests, the floor treatment was removed and steel plates were installed as the tunnel floor. The ground plane system was attached to the steel floor. The lower part of the tunnel walls were removed so that the hot gases from the nozzles could flow out beyond the test section walls and mix with cooler air before entering the downstream diffuser section. A trap-door-scavenging system was located under the ground plane. When the nozzle pressure ratios were being set, the trap door was open, allowing the hot exhaust gases to exit the test section without heating the model, ground plane, and the local environment. When the trap door was closed, the lateral flow from the nozzle jets exited the test section through the sidewall bleed system (located on both the left and right sidewalls) and thereby prevented circulation of the tunnel and jet airflow.

MODEL AND GROUND PLANE INSTRUMENTATIONS

The 9.2 percent scale model was instrumented along the underside of the fuselage, around the ramps and inlets (main and auxiliary), and also at the compressor face. The instrumentation consisted of static and total pressure probes and protruding temperature probes (which measured the surface air temperature). The main objective of this paper is to present the results at the compressor face and results showing the flow field by using a sheet laser system. Hence, the model instrumentation, other than the compressor face is shown only on the figures to which it is pertinent. Figure 10 shows the compressor face rake instrumentation, the location of each probe on the rake, and the circumferential location. Each rake arm was made up of four total pressure and five total temperature measurements. One wall static pressure tap was located by each rake arm around the circumferential. Only steady state measurements were made during this test program.

The ground plane centerline instrumentation and the ground plane rakes are shown in figure 11. The centerline instrumentation consisted of static pressures and flush-mounted thermocouples (temperature taps) which were isolated from the plate surface in order to measure the ground plane air temperature. There were three double-sided instrumented rakes and two single-sided instrumented rakes. The double-sided rakes measured the free-stream side flow and the flow coming from the nozzle jets (model side). The single-sided rakes measured only the model side of the flow. There were two rake heights, 4.0 and 11.0 in. Each rake contained total pressure, total temperature, and static pressure measurements. Additional instrumentation was located on the trap door and other section of the ground plane.

The test section airflow velocity measuring system is shown in figure 12. The propeller anemometer was located on the test section ceiling near the entrance of the test section. The anemometer could measure velocities from 1 to 98 kn within ±0.6 kn. The hot gas ingestion testing was generally conducted between velocities of 8 and 23 kn.

LASER SHEET FLOW VISUALIZATION

The flow field from the deflected thrust nozzles can be visualized by using a seeding agent, such as water, in the nozzle airflow and then intensifying the flow with a laser sheet. This laser sheet was produced by a 15-W copper vapor laser coupled with a fiber optic delivery system to take the laser beam to the test section. An optic head housing lens was coupled to the other end of the fiber cable. The lens produced a sheet of light that was approximately 18 in. high and 0.125 in. wide at the centerline of the model. The optic head was mounted on a single-axis traverse to allow remote control of the light sheet positioning and quick repositioning in the tunnel. The laser operated in the 510.6 and 578.2 nm wavelength.

To view the flow field, an array of video and still cameras were used. As many as five color video cameras were mounted at different tunnel stations in order to get the best views of the flow field and to obtain maximum light levels. The video data were recorded on 3/4-in. Umatic format and 1/2-in. VHS tape. Still photographs were taken with a combination of remotely controlled 70 mm and 35 mm cameras.

DATA ACQUISITION

The data system used for hot gas ingestion testing in the 9- by 15-ft LSWT was the NASA Lewis central data acquisition system. This system read 512 channels of pressures and 530 analog inputs (of which 440 are thermocouples), did all calculations, and displayed the results at the test facility at a rate of once per second.

Dynamic data were measured with an array of microphones for far field noise and fluctuating pressures on the fuselage, canard, and wing by using water-cooled pressure transducers able to withstand the 1460 °R exhaust nozzle airflow. These data are not a part of this paper.

TEST RESULTS

The test results are presented for a 0° splay configuration of the forward nozzles at a main landing gear height of 0.20 in. above the ground plane. The hot gas ingestion data are presented for a nozzle design pressure ratio of 1.00 on the forward nozzles and 3.16 on the aft nozzles. The compressor face Mach number was 0.40, the pitch angle was 6.5°, and the headwind velocity was 10 kn.

The effect of nozzle pressure ratio on the compressor face temperature rise is shown in figure 13 for nozzle exhaust temperatures of 960 and 1160 °R. The maximum temperature rise always occurred at the nozzle pressure ratio of 1.75; this pressure ratio corresponds to sonic condition for a single expansion ramp nozzle (SERN). The effect of increasing the exhaust temperature was an increase in compressor face temperature rise (fig. 13(a)). The effect of LID's on the compressor face temperature rise is presented in figure 13(b). The data are shown for a nozzle exhaust temperature of 960 °R for both the clean configuration and the LID's configuration. The LID's did not affect the pressure ratio (1.75) when the maximum compressor face temperature rise

occurred. However, the LID's did reduce the level of compressor face temperature rise over the range of cest nozzle pressure ratios.

The effect of nozzle exhaust temperature on the compressor face parameters at nozzle pressure ratios of 1.00 for the forward nozzles and 3.16 for the aft nozzles is presented in figure 14. The data are shown as bar graphs for simplicity. Figure 14 shows the clean configuration with nozzle exhaust temperatures of 960 and 1160 °R. The total pressure recovery was essentially unchanged. However, the total pressure distortion was about three percentage points lower at the higher temperature. The largest impact occurred on the temperature parameters - such as the temperature distortion, which increased by four percentage points, and the compressor face temperature rise, which increased by 13.6 °R.

Figure 15 contains the results from installing LID's on the undersurface of the model. LID's capture the fountain as the model descends into ground effects, hence improving the jet-induced lift. LID's also deflect the hot gas away from the inlet/fuselage region, thereby reducing the hot gas ingestion when in ground effects. The results shown in figure 15 indicate that the LID's effectively reduced the effect of HGI caused by ground effects. For example, at a nozzle exhaust temperature of 960 °R, the compressor face temperature rise was only 6 °R with LID's and 33 °R in the clean configuration. Other compressor face parameters are also generally better with LID's than the clean configuration. The total pressure recovery was 0.99 with LID's and 0.98 without LID's.

The measured inlet temperature rise variation with nozzle temperature is presented in figure 16. A limited amount of data were taken for both 98-percent and 40-percent thrust levels. The 40-percent thrust condition produced the highest inlet temperature rise. This condition is approximately the sonic condition for the SERN nozzles and tends to produce a large external near field dynamic interaction.

Since the upwash fountain interacts with the undersurface of the fuselage, the temperature distribution under the model often shows interesting distributions. Figure 17 shows the surface air temperature along the undersurface of the fuselage from the aft landing gear to the main inlet station for two nozzle exhaust temperatures. The clean configuration (fig. 17(a)), always had higher surface air temperatures over the entire length of the fuselage. The configuration with LID's (fig. 17(b)), had about the same surface air temperature as the clean configuration downstream of the LID's, station 27.50 in. However, upstream of the LID's, from station 27.50 in. through station 10.80 in., the surface air temperature was substantially reduced.

The ground plane distribution of the temperature and pressure profiles are shown in figure 18(a) and (b), respectively, for the clean configuration at nozzle exhaust temperatures of 960 and 1160 °R. In general, the temperature and pressure environments reflect the conditions encountered by the compressor face, near field and far field. The near field temperature and pressure are reflected in the ground plane centerline distance from -15 and 11 in. In this region all of the pressure changes take place, and much of the temperature rise and decay occur. The pressure field reflects that this region is under a suckdown pressure (negative) (fig. 18(b)). The surface air temperature along the ground plane, at the 10-kn headwind, forward and aft

nozzles pressure ratios of 1.00 and 3.16, respectively, remains attached through the end of the ground plane. Shown in figure 18(a) is the headwind, or ambient, temperature which is below the surface temperature distribution.

FLOW VISUALIZATION

During phase I flow visualization testing white light was used as the illuminating source and a water mist as the seeding. A typical near field view is shown in figure 19 at a headwind velocity of 10 kn and nozzle pressure ratio of 3.16. Figure 19 shows a side view of model 279-3C and the ground plane. The configuration contains the LID's. The flow from the aft nozzles can be seen impinging on the ground plane and forming the near field. Details of the flow field are lost.

During phase II, the illumination was improved by using a 15-W copper vapor laser system. The laser light was transmitted to the test section by a high-energy fiber optic cable. Water mist was used as the seeding. Figure 20 shows views of the aft nozzles at two different heights above the ground plane. The photos where taken at a headwind of 10 kn and a nozzle pressure ratio of 3.16. Figure 20(a) shows the model at a height of 12.00 in. above the ground plane. At a nozzle pressure ratio of 3.16, shock diamonds can be seen in the jet plenums. The jets also merge before striking the ground plane and form a single jet; hence there is no fountain. As the model height (main landing gear wheel height) is reduced, the jets separate before striking the ground, and an upwash fountain is formed between the two jets (fig. 20(b)). At these heights the model was in ground effects, and hot gas ingestion generally occurred. The use of the sheet laser as the illuminating source greatly improved the flow field details.

Figure 21 shows the laser sheet in the streamwise direction at a headwind velocity of 10 kn, a nozzle pressure ratio of 3.16, and a model height (main landing gear wheel height) of 0.20 in. above the ground plane. The streamwise sheet shows both the far and near flow field. The model is in ground effects, but the water mist is below the main inlet and indicates a low hot gas ingestion condition. The bright spot is the location of the upwash fountain. At a 10-kn headwind velocity, the nozzle jet flow can persist some distance ahead of the model, as shown by the laser sheet in figure 21.

A typical far field separation is shown in figure 22. The tufts on the ground plane pointing toward the model are under the influence of the headwind velocity and upstream of the far field separation zone. The tufts pointing away from the model are under the influence of the nozzle flow and are downstream of the separation zone. The tufts in the separation zone often have a 90° to 180° movement (pointing at the model to a position away from it). The influence of the ground jet was confined laterally by the headwind velocity because of the lateral velocity decay.

CONCLUDING REMARKS

The basic objectives of phase I, to develop and demonstrate STOVL hot gas ingestion (HGI) control techniques, and phase II, to extend the database for

temperature scaling and establish an air flow visualization database using a high-energy fiber optic laser sheet illumination system, were successfully met.

Both phases of the test program produced an extensive database for indepth understanding of HGI phenomena. The data will be used to improve HGI empirical prediction techniques for screening future STOVL aircraft concepts during preliminary design.

The copper vapor laser sheet illumination system provided insight into the vectored thrust flow field when the model was in and out of ground effects. In general, the characteristics of the fountain are a function of the splay angle of the forward nozzles and the height of the aircraft above the ground plane.

The NASA Lewis HGI test facility was validated as an excellent facility for accurately testing STOVL HGI. This validation established NASA Lewis as a national facility for STOVL HGI testing.

REFERENCES

1. Johns, A.L., Flood, J.D., Strock, T.W., and Amuedo, K.C., "Hot Gas Ingestion Testing of an Advanced STOVL Concept in the NASA Lewis 9- by 15-ft Low Speed Wind Tunnel With Flow Visualization," AIAA Paper 88-3025, July 1988, (Also, NASA TM-100952, 1988).

2. Johns, A.L., Neiner, G., Flood, J.D., Amuedo, K.C., and Strock, T.W., "Engine Inlet Distortion in a 9.2 Percent Scale Vectored Thrust STOVL Model in Ground Effect," AIAA Paper 89-2910, July 1989, (Also, NASA TM-102358, 1989).

3. Amuedo, K.C., Williams, B.R., Flood, J.D., and Johns, A.L., "STOVL Hot Gas Ingestion Control Technology," ASME Paper 89-GT-323, June 1989.

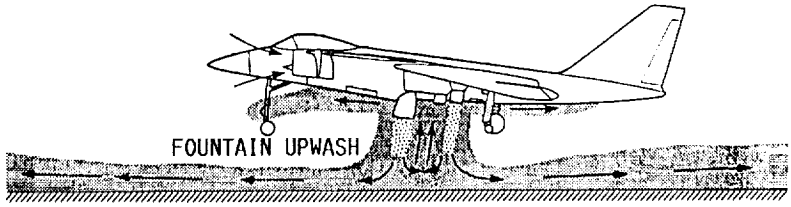

NEAR FIELD HOT GAS INGESTION DUE TO FOUNTAIN UPWASH

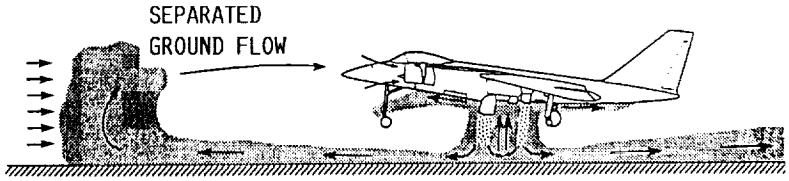

FAR FIELD HOT GAS INGESTION DUE TO SEPARATED GROUND FLOW

FIGURE 1. - SOURCES OF HOT GAS INGESTION.

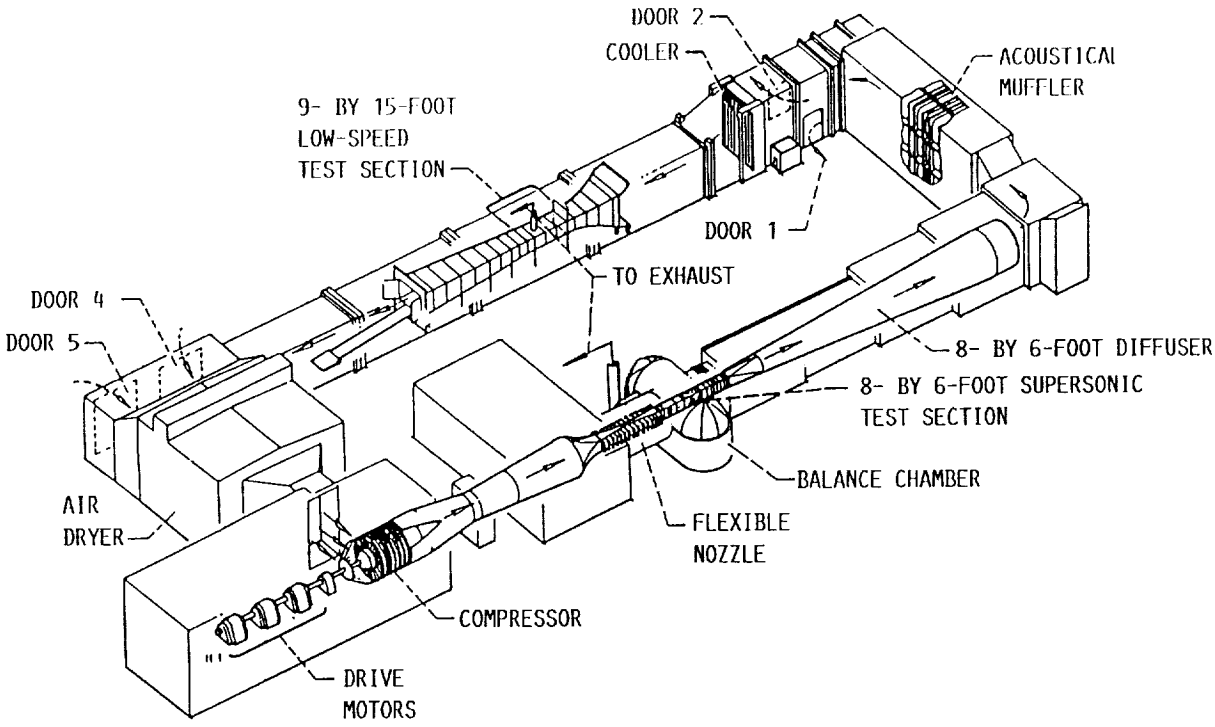

FIGURE 2. - AN ILLUSTRATION OF THE 9- BY 15-FOOT LOW-SPEED WIND TUNNEL AND THE 8- BY 6-FOOT SUPERSONIC WIND TUNNEL.

SIDE VIEW

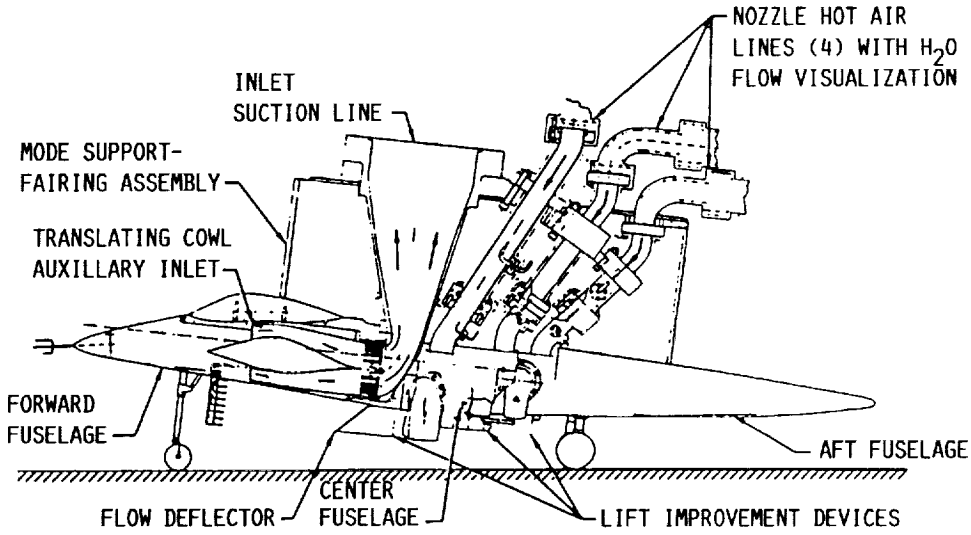

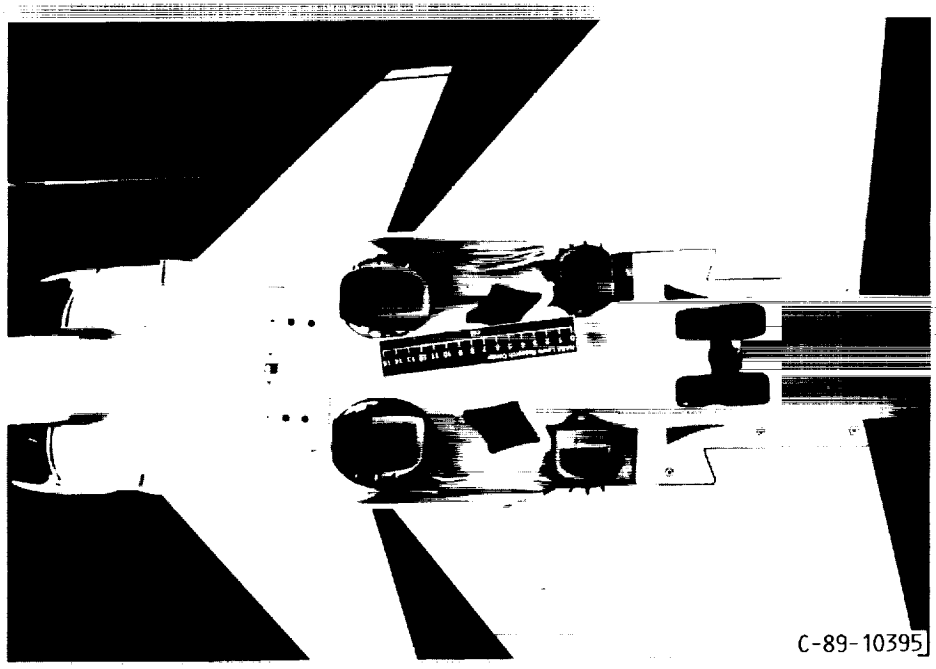

FIGURE 3. - SCHEMATIC AND UNDERSURFACE OF MODEL 279-3C.

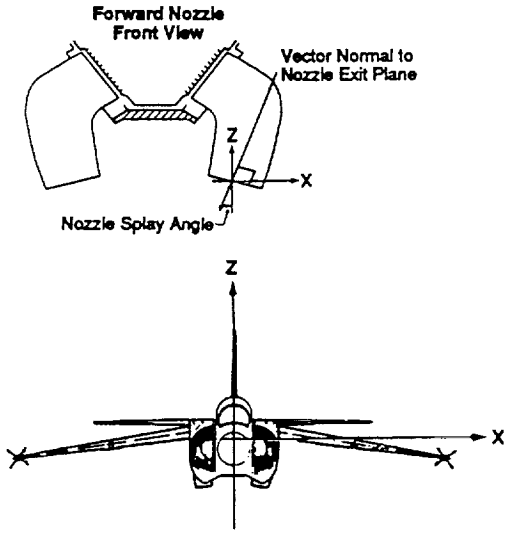

(a) NOZZLE SPLAY ANGLE.

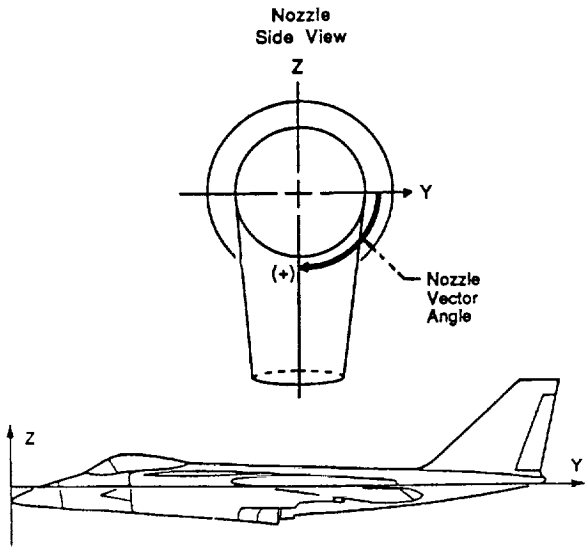

(b) NOZZLE VECTOR ANGLE.

FIGURE 4. - DEFINITION OF FORWARD NOZZLES SPLAY AND VECTOR ANGLES.

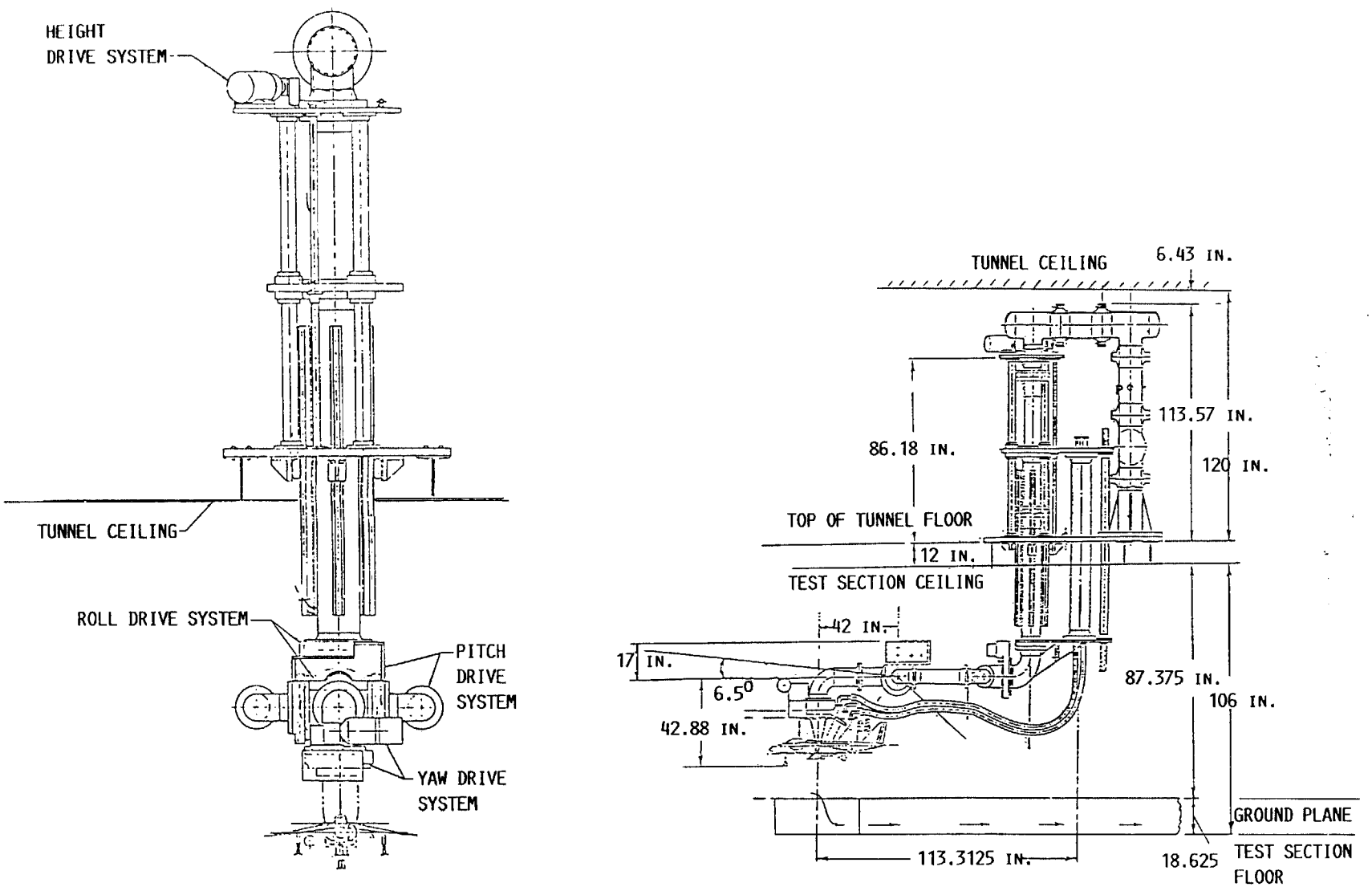

(a) FRONT VIEW.

(b) SIDE VIEW.

FIGURE 5. - MODEL INTEGRATED SUPPORT SYSTEM.

ORIGINAL PAGE
BLACK AND WHITE PHOTOGRAPH

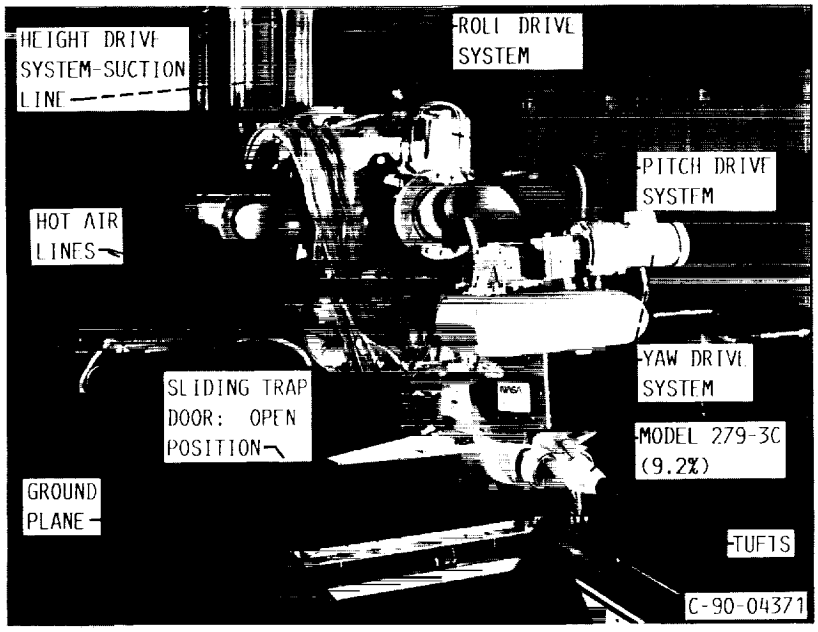

(a) MODEL AND "MISS" INSTALLATION.

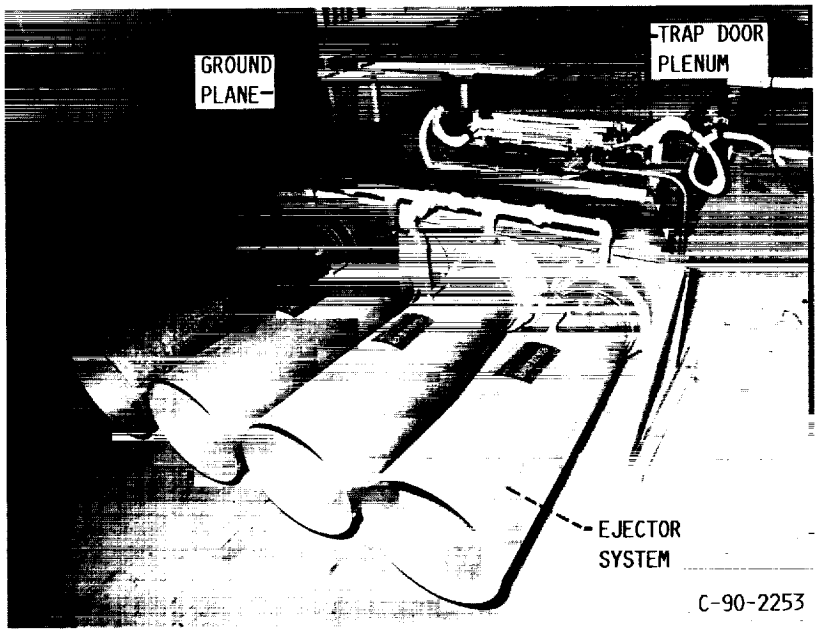

(b) AFT VIEW OF GROUND PLANE AND EJECTOR SYSTEM.

FIGURE 6. - MODEL AND "MISS" INSTALLED IN THE 9- BY 15-FOOT LOW SPEED WIND TUNNEL.

ORIGINAL PAGE
BLACK AND WHITE PHOTOGRAPH

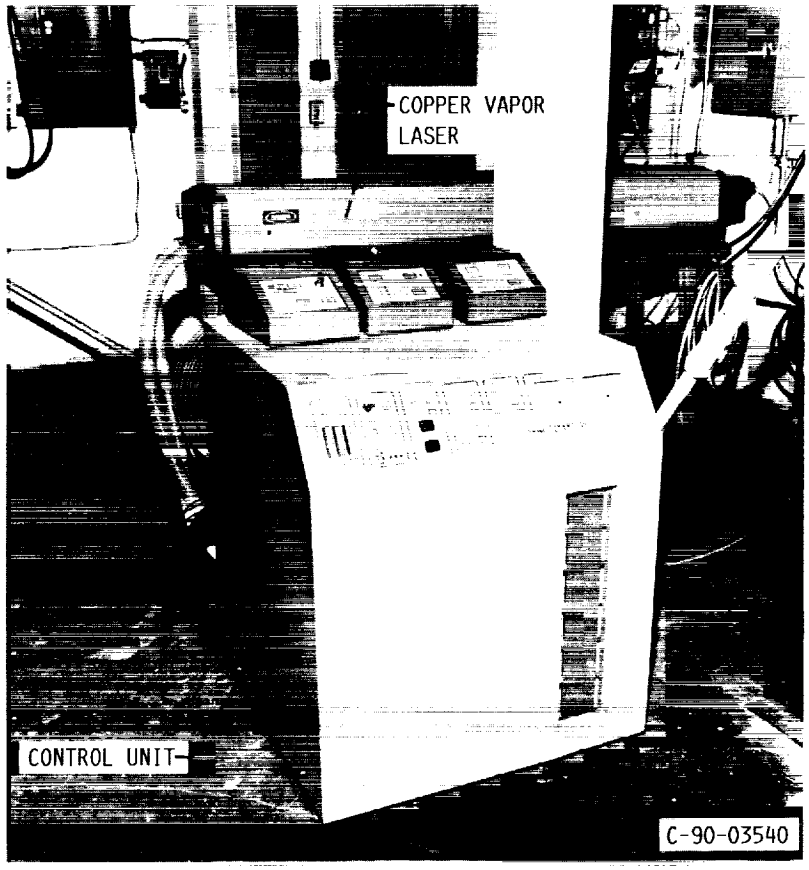

FIGURE 7. - COPPER VAPOR LASER AND CONTROL SYSTEM.

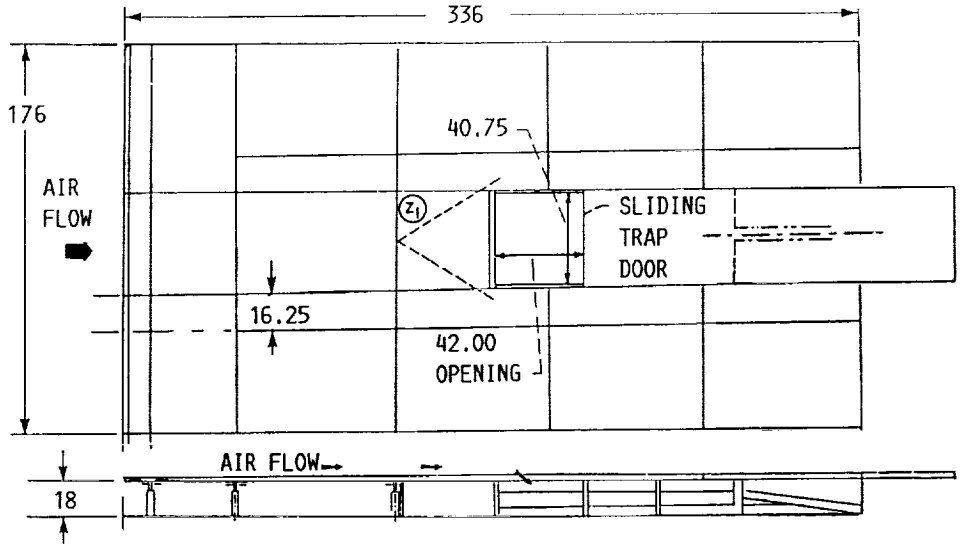

FIGURE 8. - SCHEMATIC OF THE GROUND PLANE. (DIMENSIONS IN INCHES).

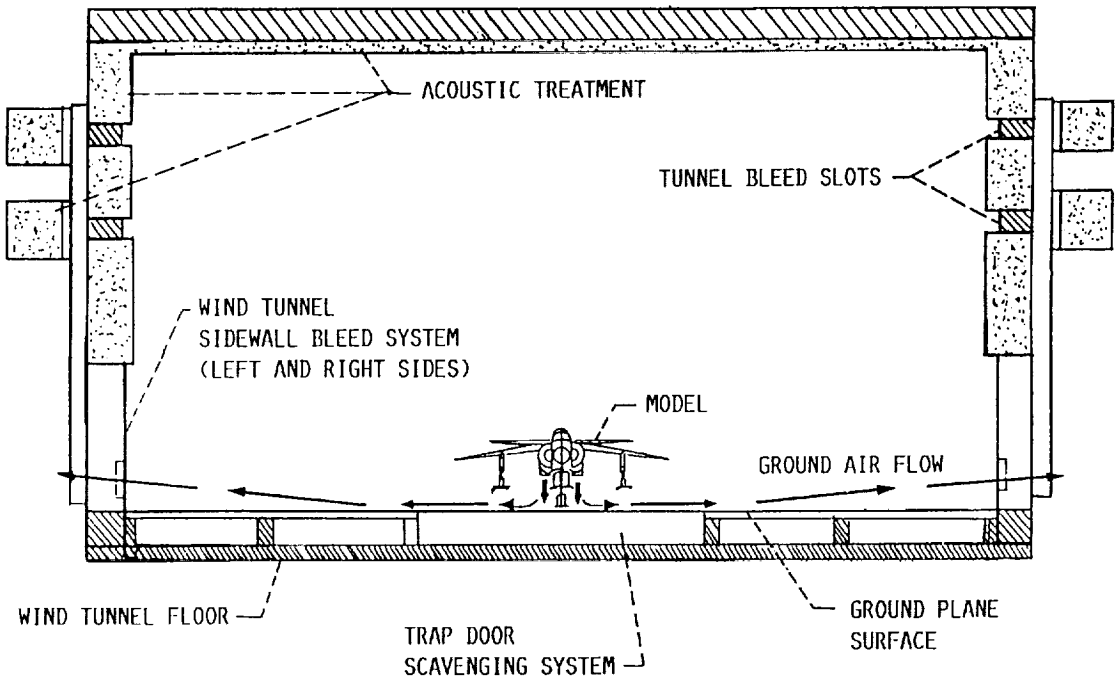

FIGURE 9. - CROSS SECTION OF THE TEST SECTION SHOWING THE SIDEWALLS BLEED AND TRAP DOOR SCAVENGING SYSTEMS.

LEG IDENTIFICATION			LEG IDENTIFICATION		
NUMBER	ANGLE, DEG	RADIUS, R, IN.	NUMBER	ANGLE, DEG	RADIUS, R, IN.
1	66.50		2	21.53	
4	293.50		3	338.47	
5	246.50		6	201.53	
8	113.50		7	158.47	
TOTAL TEMPERATURE		0.624	TOTAL TEMPERATURE		0.646
PRESSURE		0.698	PRESSURE		0.722
TEMPERATURE		1.081	TEMPERATURE		1.119
PRESSURE		1.209	PRESSURE		1.251
TEMPERATURE		1.396	TEMPERATURE		1.444
PRESSURE		1.560	PRESSURE		1.615
TEMPERATURE		1.651	TEMPERATURE		1.709
PRESSURE		1.810	PRESSURE		1.875
TEMPERATURE		1.872	TEMPERATURE		1.938
STATIC PRESSURE		2.038	STATIC PRESSURE		2.038

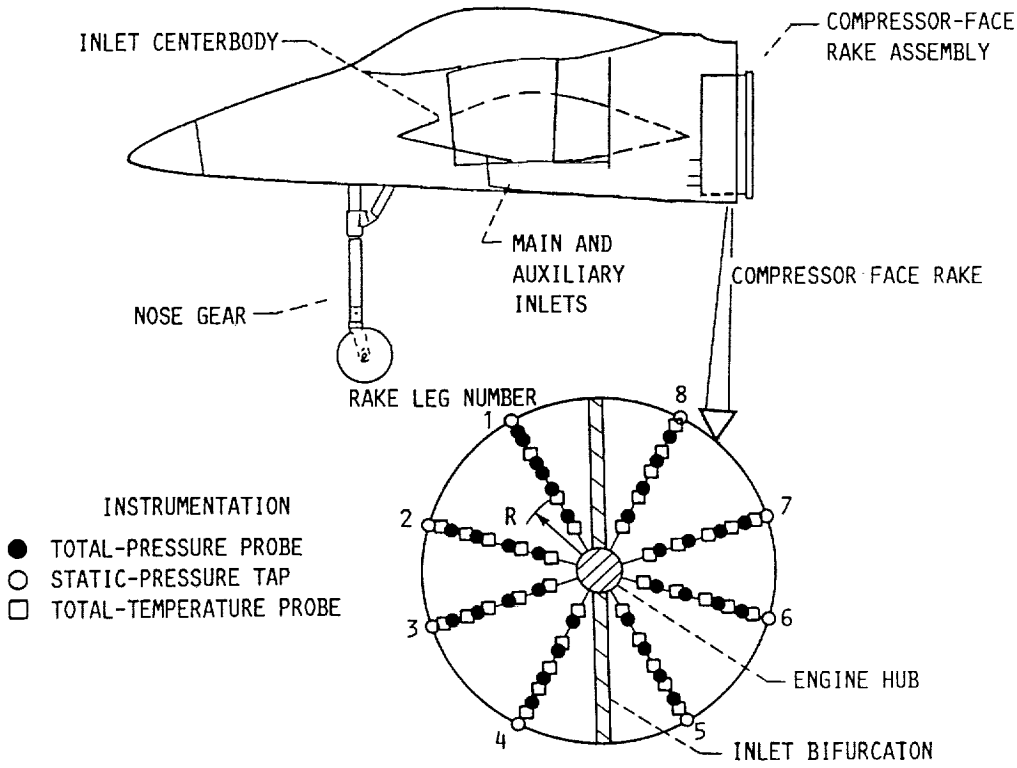

FIGURE 10. - COMPRESSOR FACE RAKE INSTRUMENTATION.

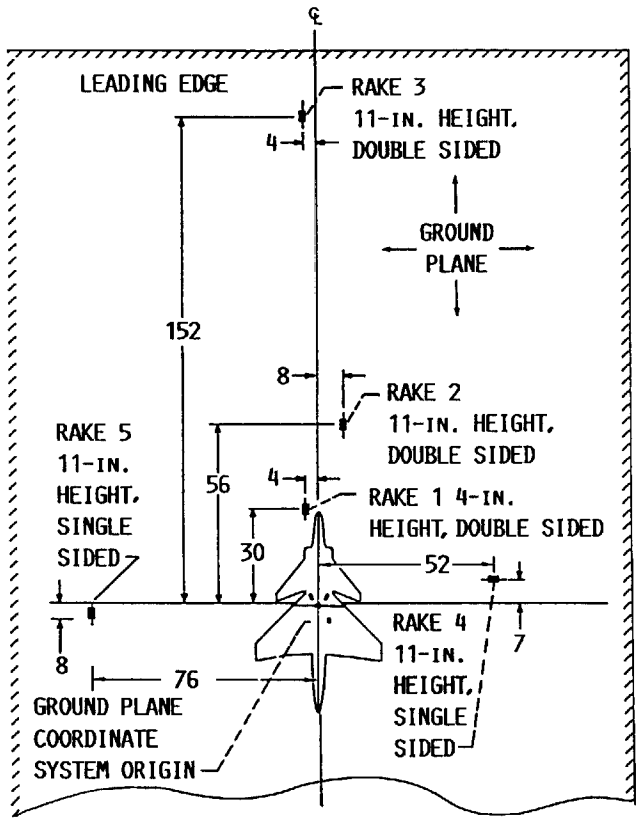

(a) STOVL MODEL.

TAP LOCATIONS, IN.

STATIC PRESSURE	SURFACE AIR TEMPERATURE
-15	-14
-13	-12
-10	-9
-8	-7
-6	-5
-4	-3
0	+1
2	3
4	5
6	7
8	9
10	11
12	13
14	15
23	24
27	28
31	34
37	40
43	46
49	52
57	58
67	
80	
92	74
104	86
117	98
122	110
128	
134	

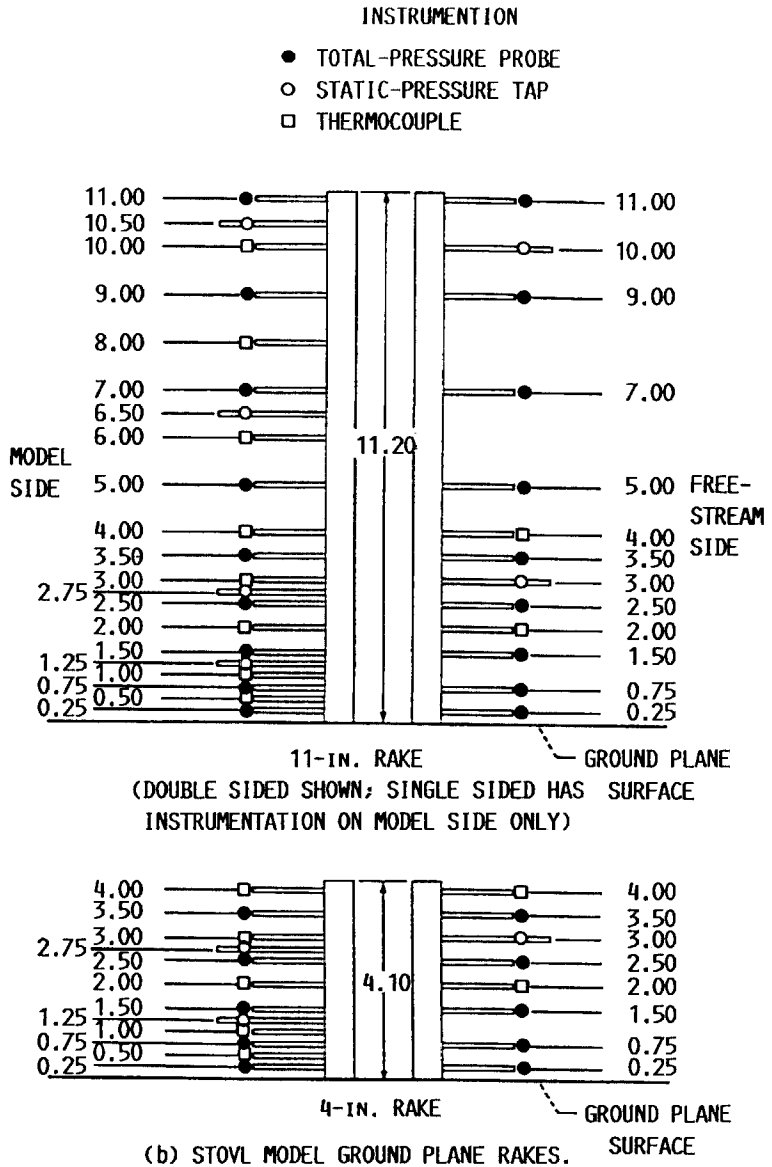

(b) STOVL MODEL GROUND PLANE RAKES.

FIGURE 11. - GROUND PLANE INSTRUMENTATION, DIMENSIONS IN INCHES.

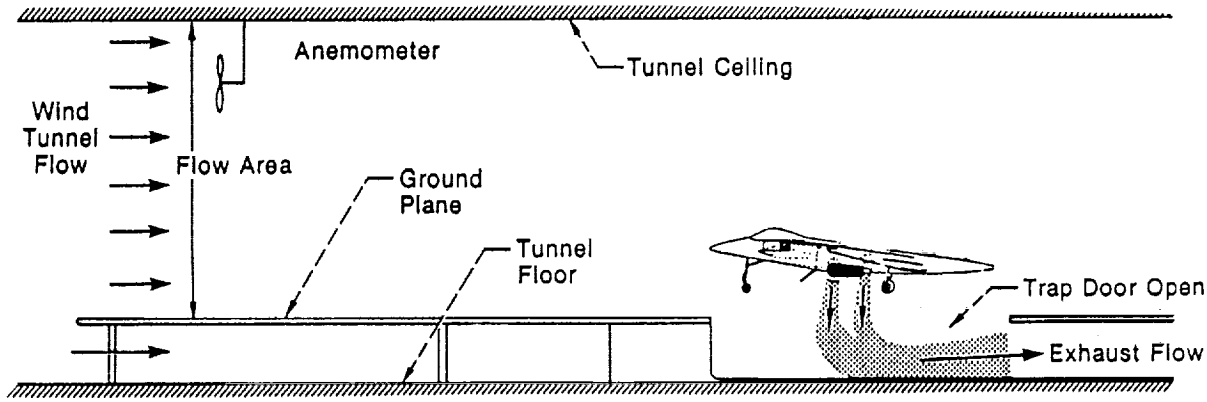

FIGURE 12. - TEST SECTION AIRFLOW VELOCITY MEASURING SYSTEM.

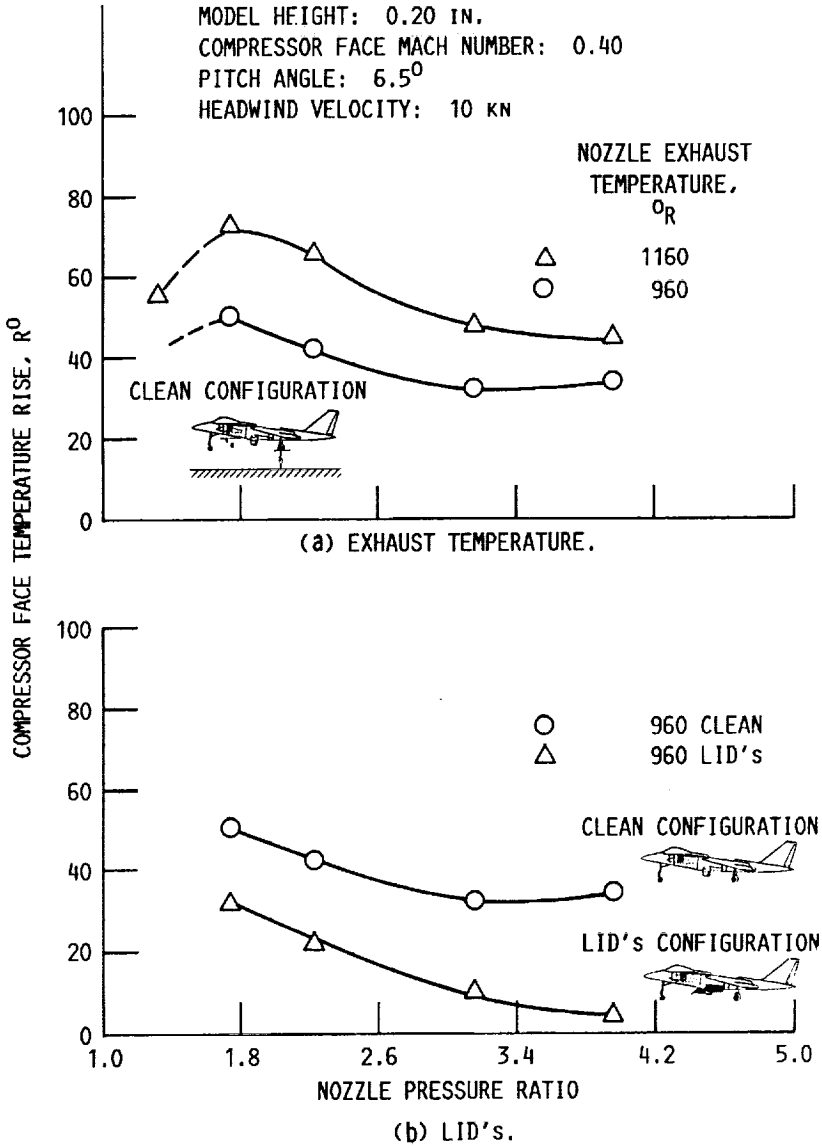

FIGURE 13. - EFFECT OF NOZZLE PRESSURE RATIO ON THE COMPRESSOR FACE TEMPERATURE RISE.

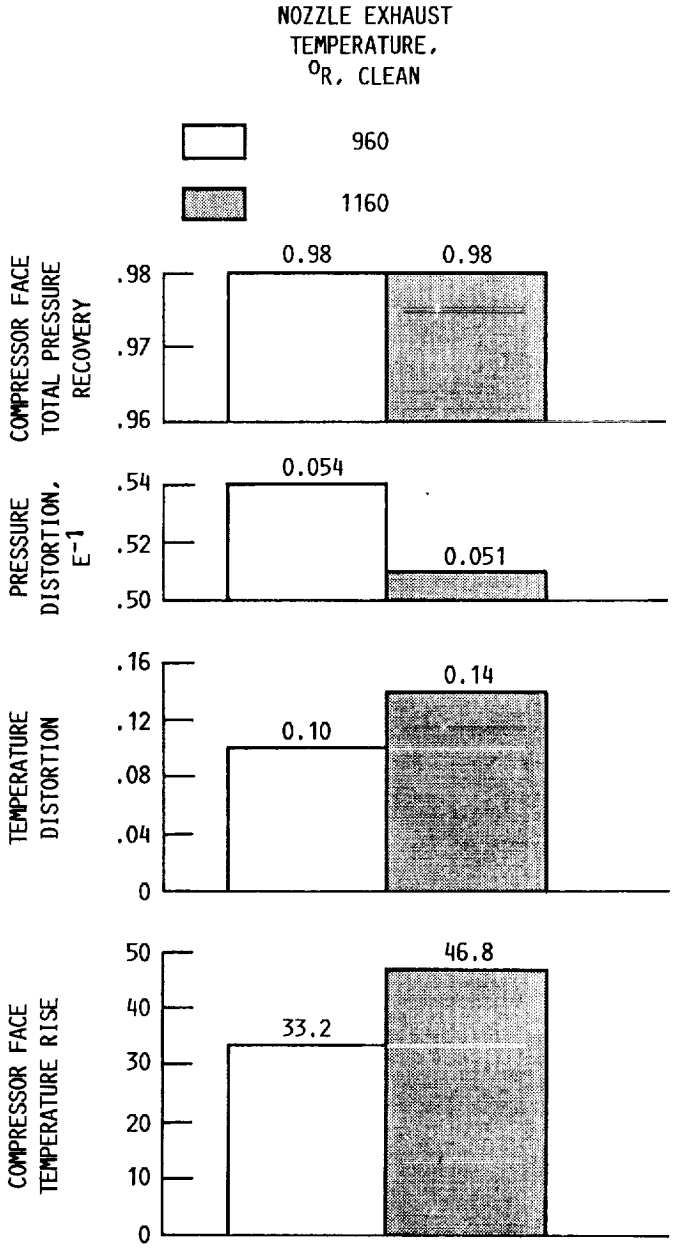

FIGURE 14. - EFFECT OF NOZZLE EXHAUST TEMPERATURE ON THE COMPRESSOR FACE PARAMETERS AT NOZZLE PRESSURE RATIOS: FORWARD NOZZLES, 1.00; AFT NOZZLES, 3.16; COMPRESSOR FACE MACH NUMBER, 0.40; PITCH ANGLE, 6.5°.

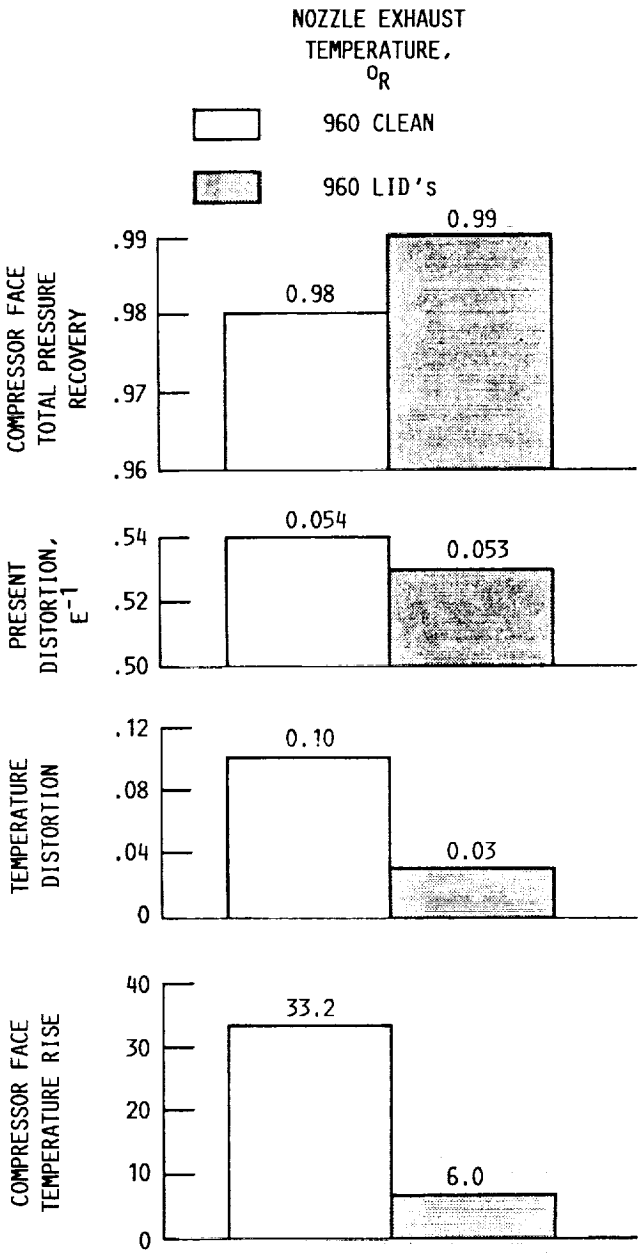

FIGURE 15. - EFFECT OF LID's ON THE COMPRESSOR FACE PARAMETERS AT NOZZLE PRESSURE RATIOS: FORWARD NOZZLES, 1.00; AFT NOZZLES, 3.16; COMPRESSOR FACE MACH NUMBER, 0.40; PITCH ANGLE, 6.5°.

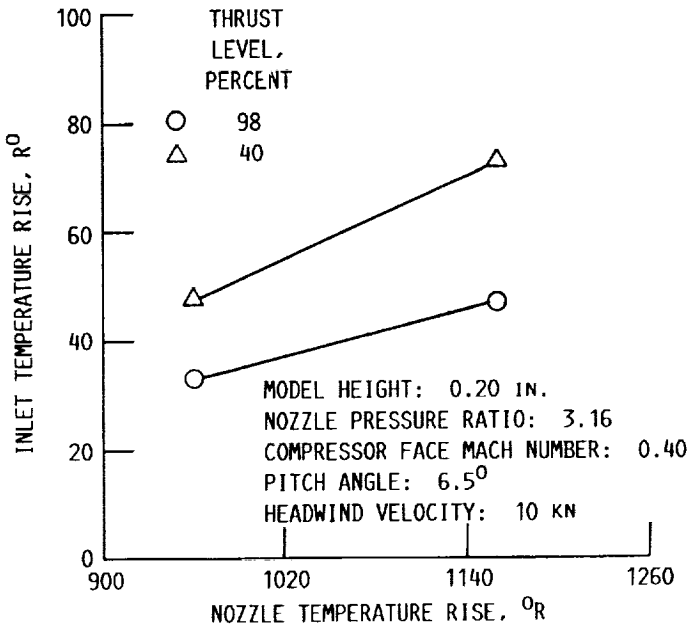

FIGURE 16. - INLET TEMPERATURE RISE VARIATION WITH NOZZLE TEMPERATURE, CLEAN CONFIGURATION.

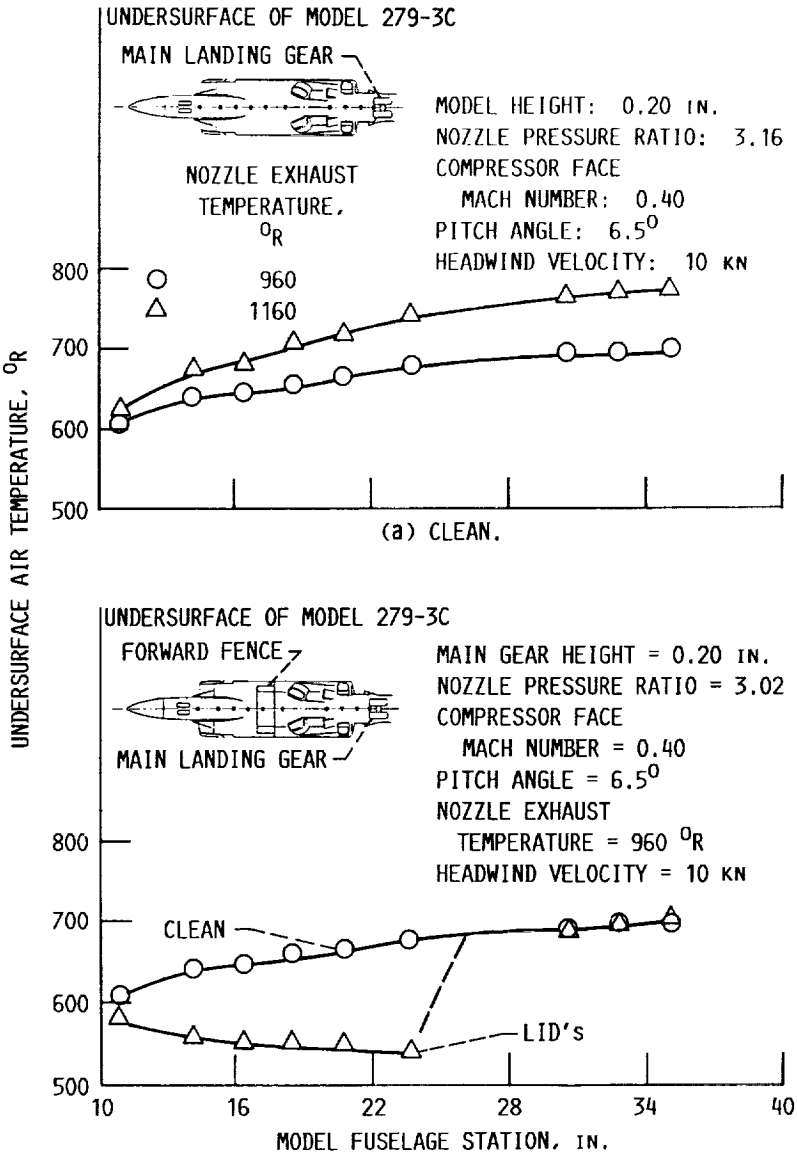

FIGURE 17. - FUSELAGE UNDERSURFACE AIR TEMPERATURE DISTRIBUTION AT 10 KN AND DESIGN NOZZLE PRESSURE RATIO.

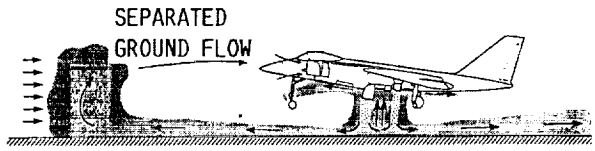

FAR FIELD HOT GAS INGESTION DUE TO SEPARATED GROUND FLOW

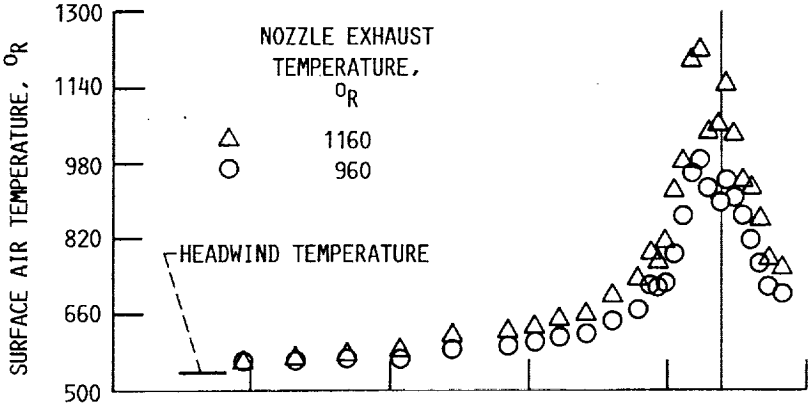

(a) SURFACE AIR TEMPERATURE.

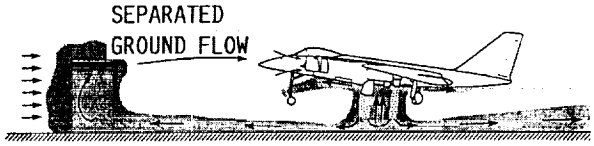

FAR FIELD HOT GAS INGESTION DUE TO SEPARATED GROUND FLOW

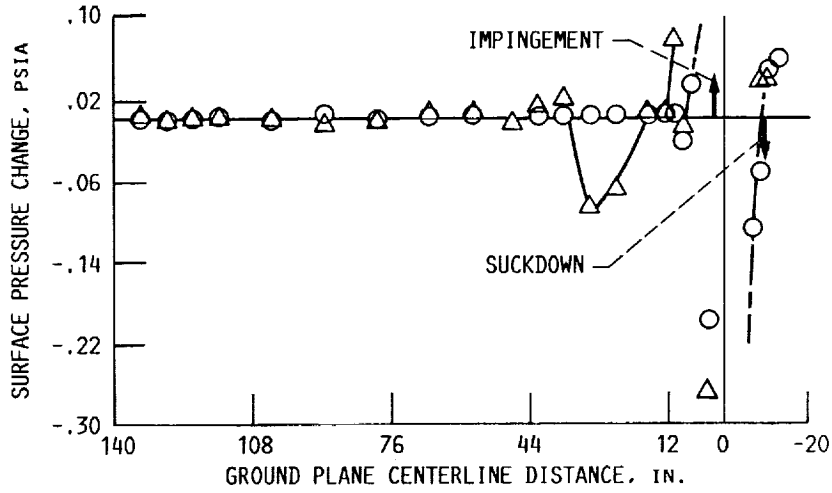

(b) SURFACE PRESSURE CHANGE.

FIGURE 18. - GROUND PLANE CENTERLINE TEMPERATURE AND PRESSURE DISTRIBUTIONS AT 10 KN AND DESIGN NOZZLE PRESSURE RATIO.

ORIGINAL PAGE
BLACK AND WHITE PHOTOGRAPH

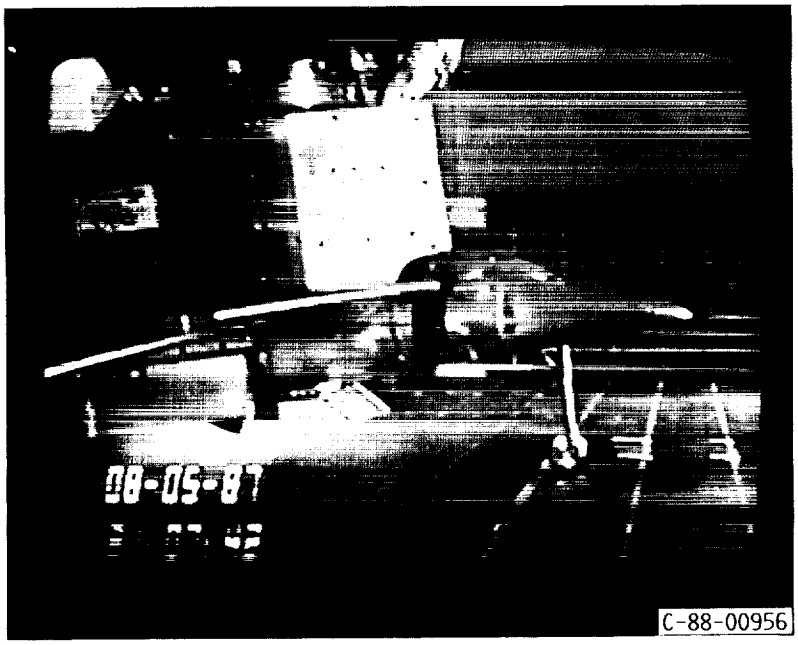

FIGURE 19. - NEAR FIELD FLOW VISUALIZATION USING WHITE LIGHT AS THE ILLUMINATING SOURCE.

ORIGINAL PAGE
COLOR PHOTOGRAPH

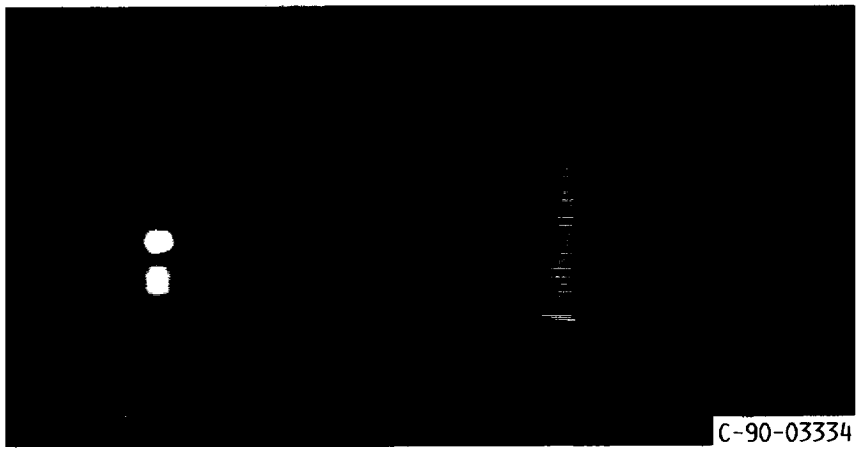

(a) MODEL HEIGHT ABOVE THE GROUND PLANE; 12.00 IN.

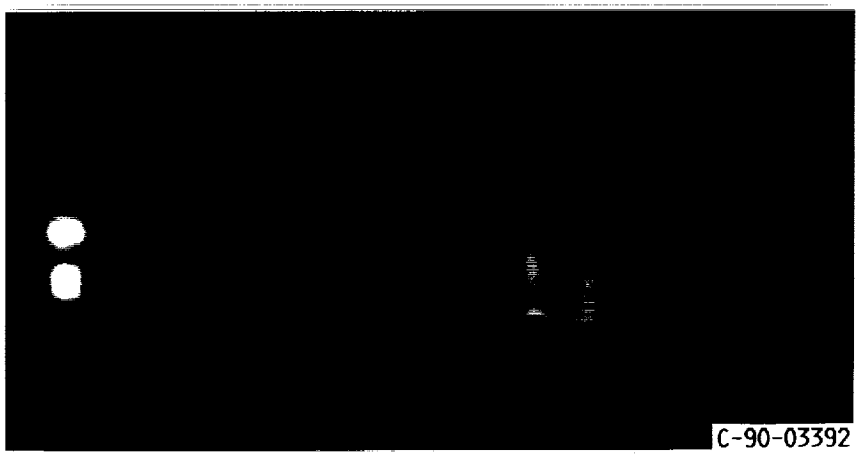

(b) MODEL HEIGHT ABOVE THE GROUND PLANE; 3.00 IN.

FIGURE 20. - NEAR FIELD FLOW VISUALIZATION USING LASER SHEET IN THE SPANWISE DIRECTION.

FIGURE 21. - FAR FIELD FLOW VISUALIZATION USING LASER SHEET IN THE STREAMWISE DIRECTION.

ORIGINAL PAGE
BLACK AND WHITE PHOTOGRAPH

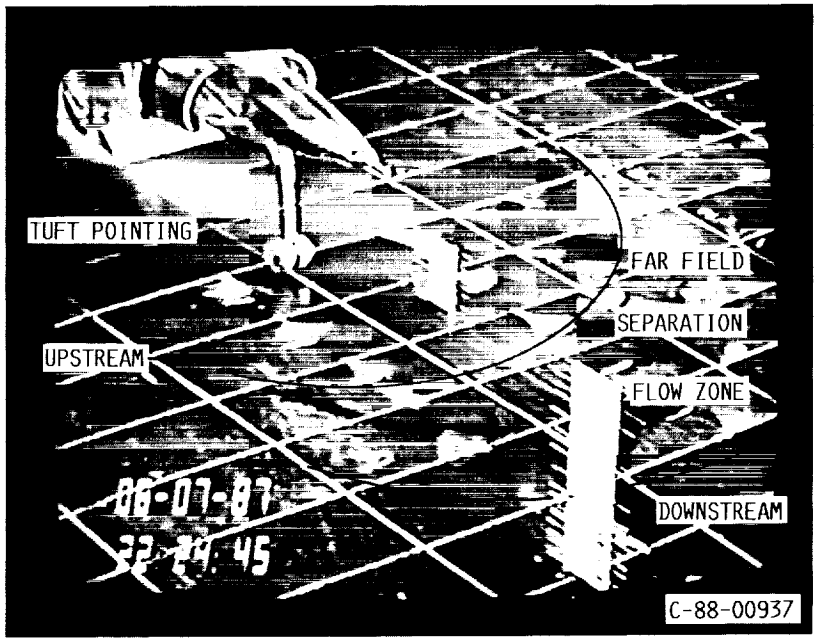

FIGURE 22. - FAR FIELD FLOW VISUALIZATION USING WHITE LIGHT AS THE ILLUMINATING SOURCE.

NASA
National Aeronautics and Space Administration

Report Documentation Page

1. Report No.	2. Government Accession No.	3. Recipient's Catalog No.
NASA TM-103258 AIAA 90-2268		

4. Title and Subtitle

Hot Gas Ingestion Test Results of a Two-Poster Vectored Thrust Concept With Flow Visualization in the NASA Lewis 9- by 15-Foot Low Speed Wind Tunnel

5. Report Date

6. Performing Organization Code

7. Author(s)

Albert L. Johns, George Neiner, Timothy J. Bencic, Joseph D. Flood, Kurt C. Amuedo, and Thomas W. Strock

8. Performing Organization Report No.

E-5690

10. Work Unit No.

505-62-71

9. Performing Organization Name and Address

National Aeronautics and Space Administration
Lewis Research Center
Cleveland, Ohio 44135-3191

11. Contract or Grant No.

13. Type of Report and Period Covered

Technical Memorandum

12. Sponsoring Agency Name and Address

National Aeronautics and Space Administration
Washington, D.C. 20546-0001

14. Sponsoring Agency Code

15. Supplementary Notes

Prepared for the 26th Joint Propulsion Conference cosponsored by the AIAA, SAE, ASME, and ASEE, Orlando, Florida, July 16-18, 1990. Albert L. Johns, George Neiner, and Timothy J. Bencic, NASA Lewis Research Center; Joseph D. Flood, Kurt C. Amuedo, and Thomas W. Strock, McDonnell Douglas Corporation, St. Louis, Missouri 63166-0516.

16. Abstract

A 9.2 percent scale Short Takeoff and Vertical Landing (STOVL) hot gas ingestion model was designed and built by McDonnell Douglas Corporation (MCAIR) and tested in the NASA Lewis Research Center 9- by 15-foot Low Speed Wind Tunnel (LSWT). Hot gas ingestion, the entrainment of heated engine exhaust into the inlet flow field, is a key development issue for advanced short takeoff and vertical landing aircraft. This paper covers flow visualization from the phase I test program, conducted by NASA Lewis and McDonnell Douglas Corporation, which evaluated the hot ingestion phenomena and control techniques. The Phase II test program, which was conducted by Lewis Research Center, evaluated the hot gas ingestion phenomena at higher temperatures and used a laser sheet to investigate the flow field. Hot gas ingestion levels were measured for the several forward nozzle splay configurations and with flow control/lift improvement devices (LID's) which reduced the hot gas ingestion. The model support system had four degrees of freedom—pitch, roll, yaw, and vertical height variation. The model support system also provided heated high-pressure air for nozzle flow and a suction system exhaust for inlet flow. The test was conducted at full scale nozzle pressure ratios and inlet Mach numbers. This paper documents test and data analysis results from Phase II and flow visualization from both Phase I and II. A description of the model and facility modifications is also provided. Headwind velocity was varied from 10 to 23 kn. Results are presented over a range of nozzle pressure ratios at a 10 kn headwind velocity. The Phase II program was conducted at exhaust nozzles temperatures up to 1460 °R and utilized a sheet laser system for flow visualization of the model flow field in and out of ground effects. The results reported herein are for nozzle exhaust temperatures up to 1160 °R. These results will contain the compressor face pressure and temperature distortions, the total pressure recovery, the inlet temperature rise, and the environmental effects of the hot gas. The environmental effects include the ground plane contours, the model airframe heating, and the location of the ground flow separation.

17. Key Words (Suggested by Author(s))	18. Distribution Statement
STOVL; Hot gas ingestion; Wind tunnel testing; Ground effects; Flow visualization; Sheet laser	Unclassified – Unlimited Subject Category 02

19. Security Classif. (of this report)	20. Security Classif. (of this page)	21. No. of pages	22. Price*
Unclassified	Unclassified	27	A03

*For sale by the National Technical Information Service, Springfield, Virginia 22161